Reduction-triggered Ligand Dissociation of Trinuclear Complex Bearing Three Kinds of Metal-ligand Units

メタデータ	言語: English 出版者: Chemical Society of Japan 公開日: 2020-03-25 キーワード (Ja): キーワード (En): Trinuclear complex, N-Heterocyclic carbene, Sulfide ligand 作成者: 籔根, 夏希, 文珠, 良侑, 中島, 洋, 西岡, 孝訓 メールアドレス: 所属: Osaka City University, Osaka City University, Osaka City University, Osaka City University
URL	https://ocu-omu.repo.nii.ac.jp/records/2019748

In April 2022, Osaka City University and Osaka Prefecture University marge to Osaka Metropolitan University

Reduction-triggered Ligand Dissociation of Trinuclear Complex Bearing Three Kinds of Metal-ligand Units

Natsuki Yabune, Ryosuke Monju, Hiroshi Nakajima,
Takanori Nishioka

Citation	Chemistry Letters. 48(12); 1511-1514-
Issue Date	2019-12-16
Type	Journal Article
Textversion	Author
Relation	The following article has been accepted by Chemistry Letters. The final, published version is available at https://doi.org/10.1246/cl.190707.
Rights	© 2019 The Chemical Society of Japan. This article may be downloaded for personal use only. Please cite only the published version.
DOI	10.1246/cl.190707

Self-Archiving by Author(s)
Placed on: Osaka City University

YABUNE, N., MONJU, R., NAKAJIMA, H., & NISHIOKA, T. (2019). Reduction-triggered Ligand Dissociation of Trinuclear Complex Bearing Three Kinds of Metal-ligand Units. *Chemistry Letters*. 48, 1511-1514. doi:10.1246/cl.190707

Reduction-Triggered Ligand Dissociation of Trinuclear Complex Bearing Three Kinds of Metal-Ligand Units

Natsuki Yabune, Ryosuke Monju, Hiroshi Nakajima, and Takanori Nishioka*
Department of Chemistry, Graduate School of Science, Osaka City University, Osaka 558-8585

E-mail: nishioka@sci.osaka-cu.ac.jp

A heterometallic trinuclear complex with three metal-metal bonds, which is constituted of three kinds of metal-ligand units bridged by two sulfido ligands, reacts with a 2-electron donor to afford an adduct accompanied with elongation of the metal-metal bonds. Cyclic voltammograms of the complexes showed that the adduct releases the 2-electron donor after electrochemical 1-electron reduction.

Keywords: Trinuclear complex, N-Heterocyclic carbene, Sulfide ligand

Trinuclear complexes with 48 cluster valence electrons (CVEs) are stable and relatively unreactive because of closed-shell electron configuration of metal centers with three metal-metal bonds.[1] Even though, some reactions such as substitution[2–12] and addition[13] were reported. For example, one carbonyl ligand of Co_2Fe carbonyl clusters substituted with phosphines or arsines with no change of the CVEs.[2–5] An Ir_2M complexes (M = Pd, Pt) also showed similar substitution reaction on the Pd or Pt center, of which chloro ligands were substituted with pyridine derivatives[6] or phosphines.[7] Successive addition of CO ligands to a $CrMn_2$ carbonyl clusters resulted in M–M bond elongation with CVE changes from 48 to 50 and from 50 to 52.[13] A Ru_3 complex with 48 CVEs exhibited reversible thermal activation of a P–C bond in one of two PPh_3 ligands in the complex.[14] For a Co_2Fe carbonyl cluster with a triply bridging sulfido ligand, isolobal displacement reaction with Cr carbonyl complexes with substituted cyclopentadienyl ligands was also reported.[15]

We previously reported trinuclear complexes bearing triply bridging sulfido ligands, $[(MCp^*)_3(\mu_3\text{-}S)_2]^{2+}$ (M = Rh, Ir; Cp* = η^5-C_5Me_5).[16] The complexes are very stable and reduction of the complexes promotes reaction with CO_2 via M–M or M–S bond cleavage.[17–19] We also synthesized M₂M’ type trinuclear complexes $[(MCp^*)_2\{Pt(bisNHC\text{-}Cn)\}(\mu_3\text{-}S)_2]^{2+}$ (M = Rh, Ir; M’ = Pd, Pt; bisNHC-C*n* = $(CH_2)_n$-bridged bis(N-substituted-imidazolylidene), *n* = 1–3) to tune properties of trinuclear complexes by replacement of one of the three {Cp*M} moieties in $[(MCp^*)_3(\mu_3\text{-}S)_2]^{2+}$ with one {M’(bisNHC-C*n*)} unit, which are electronically and stereochemically tunable components using variable N-substituents and the alkylene bridges.[20,21] Here, we planned to replace one more {MCp*} moiety with a {Pt(bpy)} unit and report sequential construction of a (ML)(M’L’)(M’L”) type trinuclear complex with triply-bridging sulfido ligands with 48 CVEs. We also describe the reaction of the 48-CVE complex with triethyphosphite as a 2-electron donor affording a complex with 50 CVEs, which releases the phosphite ligand via electrochemical reduction of the complex.

A 48-CVE heterometallic trinuclear complex constituted of three metal-ligand units, $[\{Pt(bisNHC)\}\{Pt(bpy)\}(RhCp^*)(\mu_3\text{-}S)_2]^{2+}$ ($[\mathbf{2}]^{2+}$, bisNHC = methylene-bridged bis(N-methylimidazolylidene)), was synthesized via addition of the {Pt(bpy)} unit to a dinuclear complex $[\{Pt(bisNHC)\}\{RhCp^*[P(OEt)_3]\}(\mu\text{-}SH)_2]^{2+}$ ($[\mathbf{1}]^{2+}$), which was obtained from the reaction of in-situ generated $[RhCp^*\{P(OEt)_3\}(SH)_2]$ with $[Pt(bisNHC)(NCMe)_2]^{2+}$. The 48-CVE PtPtRh complex reacts with triethyl phosphite to afford a corresponding 50-CVE adduct, $[\{Pt(bisNHC)\}\{Pt(bpy)\}\{RhCp^*[P(OEt)_3]\}(\mu_3\text{-}S)_2]^{2+}$ ($[\mathbf{3}]^{2+}$), which releases the phosphite ligand by heating to lead regeneration of the 48-CVE complex (Scheme 1).

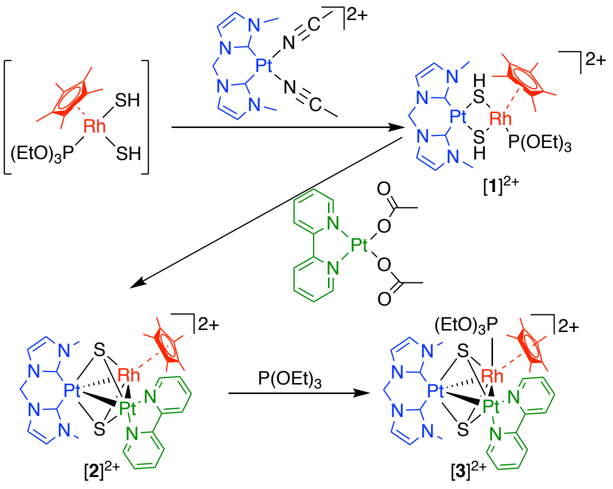

Scheme 1. Syntheses of dinuclear and trinuclear complexes

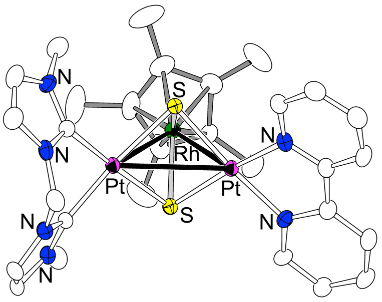

Figure 1. Structure of the cationic moiety of the PF_6 salt of 48-CVE PtPtRh complex $[\mathbf{2}](PF_6)_2$. Hydrogen atoms are omitted for clarity.

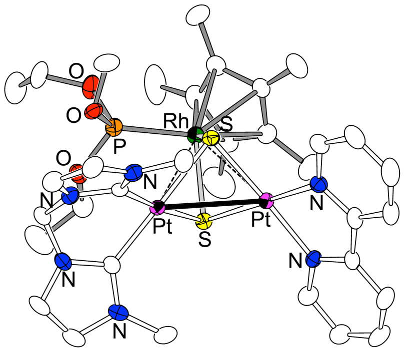

Figure 2. Structure of the cationic moiety of the PF_6 salt of 50-CVE PtPtRh complex $[\mathbf{3}](PF_6)_2$. Hydrogen atoms are omitted for clarity.

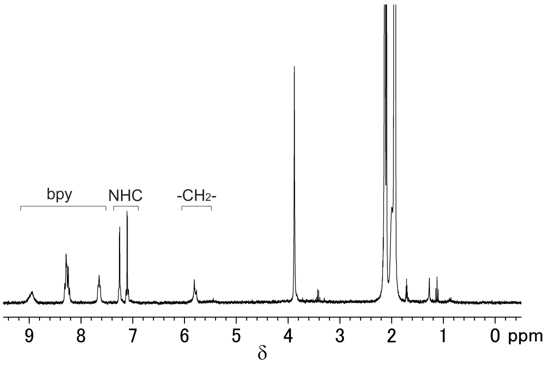

Figure 3. ^1H NMR spectrum in CD_3CN for 48-CVE complex $[\mathbf{2}]^{2+}$.

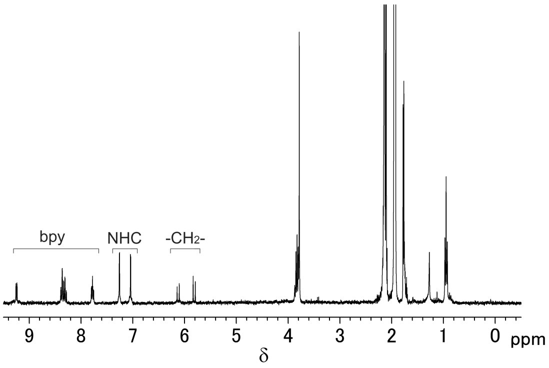

Figure 4 ^1H NMR spectrum in CD_3CN for 50-CVE complex $[\mathbf{3}]^{2+}$.

The structures of the hexafluorophosphate salts of 48- and 50-CVE complexes $[\mathbf{2}](PF_6)_2$ and $[\mathbf{3}](PF_6)_2$, respectively, were analyzed by using X-ray crystallography (Figures 1 and 2).[22,23] In each complex, three metal ions are bridged by two sulfido ligands and two platinum(II) ions adopt square planer geometry when the metal-metal bonds are not taken into account. Complex $[\mathbf{2}]^{2+}$ involves formally five-coordinated rhodium(III) ion with two sulfido and one Cp * ligands, and $[\mathbf{3}]^{2+}$ contains formally six-coordinated rhodium(III) ion with piano stool type geometry constituted of one Cp*, two sulfido and one phosphite ligands. Although there are two possible isomers for $[\mathbf{2}]^{2+}$ due to the orientation of the bisNHC ligand adopting a bent structure, only one of them was observed in the crystallographic analysis. ^1H NMR spectrum of the complex (Figure 3) showed broad signals despite of the diamagnetic nature of the 48-CVE cluster core in $[\mathbf{2}]^{2+}$. This broadening of the signals is attributed to the wing-flapping motion of the bisNHC ligand, which was reported for heterometallic M_2M' type trinuclear complexes, $[(MCp^*)_2\{M'(bisNHC)\}(\mu_3\text{-}S)_2]^{2+}$ (M = Rh, Ir; M' = Pd, Pt).[21] This means that there are two isomers in solution and one of them crystallizes probably due to the difference in solubility and/or crystal packing effects of the isomers. On the other hand, ^1H NMR spectrum of $[\mathbf{3}]^{2+}$ (Figure 4) showed only one set of sharp signals for the complex even though there are four possible isomers occurred by the orientation of the bisNHC ligand and location of the phosphite ligand. This result suggests that only one isomer exists in solution. This selective formation of the complex is probably attributed to steric repulsion between the ancillary ligands of the metal-ligand units and the phosphite ligand. The Rh–Pt distances significantly elongate by the coordination of the phosphite ($Rh\text{–}Pt_{NHC}$ and $Rh\text{–}Pt_{bpy}$; 2.9985(9) and 2.8977(8) Å for $[\mathbf{2}]^{2+}$ and 3.3796(6) and 3.3326(6) Å for $[\mathbf{3}]^{2+}$, respectively) while the Pt–Pt distance shortens (3.204(1) and 2.9970(5) Å for $[\mathbf{2}]^{2+}$ and $[\mathbf{3}]^{2+}$, respectively). This fact implies that the bond orders for two of three metal-metal bonds in $[\mathbf{2}]^{2+}$ decrease from 1 to 0.5 by the coordination of the two-electron donor rather than one of the three metal-metal bonds in $[\mathbf{2}]^{2+}$ is cleaved via changing CVEs from 48 for $[\mathbf{2}]^{2+}$ to 50 for $[\mathbf{3}]^{2+}$ by the coordination of the phosphite.

The cyclic voltammogram (CV) for $[\mathbf{2}]^{2+}$ (Figure 5, blue line) exhibited two reversible 1-electron reduction/re-oxidation couples at –1.34 ((a)/(d)) and –1.80 V ((b)/(c)) vs. Fc^+/Fc. DFT calculation of the complex suggested that the reduction occurred at the cluster core (See Supporting Information). Similar redox behavior of 48-CVE trinuclear complexes with triply bridging sulfido ligands were reported for $[\{Pt(bisNHC)\}(RhCp^*)_2(\mu_3\text{-}S)_2]^{2+}$ and $[(RhCp^*)_3(\mu_3\text{-}S)_2]^{2+}$ showing two reversible redox couples at –1.10 and –1.67 V[16,17] and –0.90 and –1.29 V,[20,21] respectively. The redox potentials for PtPtRh complex $[\mathbf{2}]^{2+}$ are more negative than those observed for the Rh_3 and $PtRh_2$ complexes.

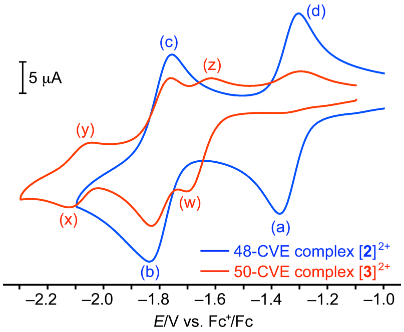

Figure 5. Cyclic voltammograms for 48- ($[\mathbf{2}]^{2+}$, 0.5 mM, blue line) and 50-CVE ($[\mathbf{3}]^{2+}$, 0.5 mM, red line) PtPtRh complexes. 0.1 M $TBAPF_6$ in MeCN. Scan rate: 100 mV/s. Working electrode: ϕ3 mm glassy carbon.

On the other hand, phosphite-coordinated 50-CVE complex $[\mathbf{3}]^{2+}$ showed a complicated voltammogram (Figure

5, red line). Other than two quasi-reversible couples ((w)/(z) and (x)/(y)), the CV exhibited the waves corresponding to the redox processes for 48-CVE complex $[\mathbf{2}]^{2+}$ ((b), (c) and (d)) probably due to a subsequent reaction. To confirm such EC process, faster scan rate (5000 mV/s) was applied for the measurement affording a simple voltammogram showing only the two quasi-reversible couples, (w)/(z) and (x)/(y), which correspond to $[\mathbf{3}]^{2+/+}$ and $[\mathbf{3}]^{+/0}$ redox couples, respectively (Figure 6). DFT calculation of the complex implies that the reduction occurred at the {Pt(bpy)} unit (See Supporting Information). The observation of the redox waves (b), (c), and (d) corresponding to the redox series for $[\mathbf{2}]^{2+}$ in the CV of $[\mathbf{3}]^{2+}$ with the slower scan rate (Figure 5, red line) shows that the subsequent reaction gives phosphite-dissociated complex $[\mathbf{2}]^{+}$. The appearance of the re-reduction wave (a) in the second cathodic scan in the CV with repeated scan cycles (Figure 7) also supports the formation of 48-CVE complex $[\mathbf{2}]^{2+}$. Ligand-dissociation enhanced by electrochemical reduction was reported for a triiron carbonyl complex with triply bridging sulfido ligands.[24]

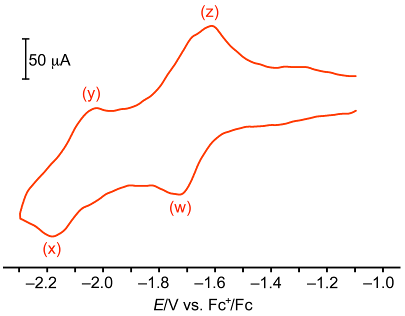

Figure 6. Cyclic voltammogram for 50-CVE PtPtRh complex ($[\mathbf{3}]^{2+}$, 0.5 mM). 0.1 M $TBAPF_6$ in MeCN. Scan rate: 5000 mV/s. Working electrode: ϕ3 mm glassy carbon.

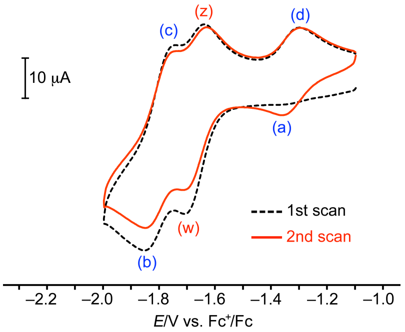

Figure 7. Cyclic voltammograms with repeated scans for 50-CVE complex $[3]^{2+}$ (0.5 mM). 0.1 M $TBAPF_6$ in MeCN. Scan rate: 100 mV/s. Working electrode: ϕ3 mm glassy carbon (dashed line: 1st scan, red line: 2nd scan).

The CV measurement of phosphite-coordinated complex $[3]^{2+}$ in the presence of excess phosphite was also performed (Figure 8) because the disappearance of the waves for the redox series of the phosphine-dissociated complex $[2]^{2+}$ was expected due to its reaction with excess phosphite. However, the CV exhibited no re-oxidation wave for $[\mathbf{3}]^{2+/+}$ even the waves (b), (c), and (d) for the redox series of $[\mathbf{2}]^{2+}$ were observed. This result implies that 1-electron reduced complex $[\mathbf{3}]^{+}$, which partially remained after slow dissociation reaction of the $P(OEt)_3$ ligand in the EC process, would react with excess phosphite and decompose to the other complexes. Observation of the waves (b), (c), and (d) also suggests that the reaction of the phosphite-released 49- and 50-CVE complexes with $P(OEt)_3$ is slow because no re-oxidation wave for the phosphite-coordinated complex was observed. The electrochemical processes described in this paper are summarized in Scheme 2. The labels (a)–(d) and (w)–(z) are corresponding to the redox waves labeled in Figures 5–8.

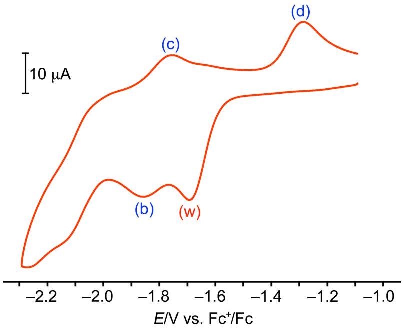

Figure 8. Cyclic voltammogram for 50-CVE complex ($[\mathbf{3}]^{2+}$, 0.5 mM) in the presence of excess $P(OEt)_3$. 0.1 M $TBAPF_6$ in MeCN. Scan rate: 100 mV/s. Working electrode: ϕ3 mm glassy carbon.

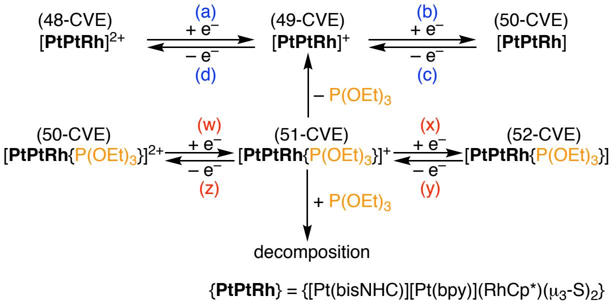

Scheme 2. Electrochemical processes for a redox series of 50- and 48-CVE complexes, $[3]^{\cdot+}$ and $[2]^{2+}$.

In conclusion, we demonstrated rational synthesis of the 48-CVE PtPtRh heterometallic trinuclear complex constituted of three kinds of metal-ligand units, $[\{Pt(bisNHC)\}\{Pt(bpy)\}(RhCp^*)(\mu_3\text{-}S)_2]^{2+}$, by sequential construction via the PtRh dinuclear complex, $[\{RhCp^*[P(OEt)_3]\}[Pt(bisNHC)](\mu\text{-}SH)_2]^{2+}$, in relatively high total yield. The 48-CVE trinuclear complex, which possesses a five-coordinated Rh center, readily reacts with triethyl phosphite as a 2-electron donor to afford the 50-CVE complex, $[\{Pt(bisNHC)\}\{Pt(bpy)\}\{RhCp^*[P(OEt)_3]\}(\mu_3\text{-}S)_2]^{2+}$, in which the phosphite ligand coordinates to the Rh center bearing a pseudo-octahedral geometry with one Cp*, two sulfido and one phosphite ligands. While the 48-CVE complex showed two reversible redox couples in a cathodic sweep in cyclic voltammetry, the 50-CVE complex exhibited a subsequent reaction of dissociation of the phosphite ligand following the 1-electron reduction to 51-CVE complex. Re-oxidation of the resulted phosphine-dissociated 49-CVE complex regenerates the 48-CVE complex. These results would provide new insights of reactivity and nature of metal-metal bonding in redox active multinuclear complexes for utilization of such clusters as redox active catalysts and molecular sensing materials. Syntheses of related 48-CVE complexes with different combination of metal-ligand units, $[\{M(bisNHC)\}\{M(bpy)\}(M'Cp^*)(\mu_3\text{-}S)_2]^{2+}$ (M = Pd or Pt; M' = Rh or Ir), and investigation of the details of reactions with phosphite or other 2-electron donors such as CO to elucidate the relation between metal-ligand units in trinuclear complexes and their chemical and electrochemical properties is in progress.

This work was partly supported by JSPS KAKENHI Grant Number JP17K05814.

Supporting Information is available on http://dx.doi.org/10.1246/cl.******.

References and Notes

1 P. Atkins, T. Overton, J. Rourke, M. Weller, F. Armstrong, in *Shriver & Atkins Inorganic Chemistry*, 4th ed., Oxford University Press, Oxford, U.K., **2006**, pp 557–558.

2 P. Zhao, X.-F. Liu, H.-K. Wu, *J. Coord. Chem.* **2017**, *70*, 3080-3094.

3 R. M. De Silva, M. J. Mays, P. R. Raithby, G. A. Solan, *J. Organomet. Chem.* **2002**, *642*, 237–245.

4 W. Gao, *Asia J. Chem.* **2015**, *9*, 3515–3516.

5 W. Gao, *Asia J. Chem.* **2015**, *9*, 3517–3518.

6 T. Fujimura, H. Seino, M. Hidai, Y. Mizobe, *J. Organomet. Chem.* **2004**, *689*, 738–743.

7 D. Masui, T. Kochi, Z. Tang, Y. Ishii, Y. Mizobe, M. Hidai, *J. Organomet. Chem.* **2001**, *620*, 69–79.

8 F.-E. Hong, S.-C. Chen, Y.-T. Tsai, Y.-C- Chang, *J. Organomet. Chem.* **2001**, *655*, 172–181.

9 F.-E. Hong, C.-P. Chang, H. Chang, Y.-L. Huang, Y.-C- Chang, *J. Organomet. Chem.* **2003**, *677*, 80–88.

10 A. R. Manning, A. J. Palmer, *J. Organomet. Chem.* **2002**, *651*, 60–65.

11 T. Kochi, Y. Nomura, Z. Tang, Y. Ishii, Y. Mizobe, M. Hidai, *J. Chem. Soc., Dalton Trans.* **1999**, 2575–2582.

12 A. L. Eckermann, D. Fenske, T. B. Rauchfuss, *Inorg. Chem.* **2001**, *40*, 1459–1465.

13 M, Shieh, C.-H. Yu, Y.-Y. Chu, Y.-W. Guo, C.-Y. Huang, K.-J. Hsing, P.-C. Chen, C.-F. Lee, *Chem. Asian J.* **2013**, *8*, 963–973.

14 J. A. Cabeza, I. del Río, V. Riera, *Organometallics*, **1997**, *16*, 1743–1748.

15 L.-C. Song, H.-W. Cheng, Q.-M. Hu, Z. Wang, *J. Organomet. Chem.* **2004**, *689*, 139–145.

16 T. Nishioka, K. Isobe, *Chem. Lett.* **1994**, 1661-1664.

17 Y. Kushi, H. Nagao, T. Nishioka, K. Isobe, K. Tanaka, *Chem. Lett.* **1994**, 2175-2178.

18 Y. Kushi, H. Nagao, T. Nishioka, K. Isobe, K. Tanaka, *J. Chem. Soc., Chem. Commun.* **1995**, 1223-1224.

19 K. Tanaka, Y. Kushi, K. Tsuge, K. Toyohara, T. Nishioka, K. Isobe, *Inorg. Chem.* **1998**, *37*, 120-126.

20 Y. Maeda, H. Hashimoto, I. Kinoshita, T. Nishioka, *Inorg. Chem.* **2015**, *54*, 448-459.

21 Y. Maeda, H. Hashimoto, I. Kinoshita, T. Nishioka, *Inorg. Chem.* **2014**, *53*, 661-663.

22 Crystallographic data for [**2**]$(PF_6)_2$: $C_{29}H_{35}F_{12}N_6P_2Pt_2RhS_2$, M_r = 1314.77, triclinic, $P\bar{1}$, a = 9.547(3), b = 13.220(5), c = 15.519(5) Å, α = 78.196(12), β = 80.820(13), γ = 89.595(14)°, V = 1892.0(11) Å^3, Z = 2, D_{calcd} = 2.308 g cm^{-3}, 13708 total reflections, 7927 unique (R_{int} = 0.0432), $R1$ = 0.0434 [$I > 2\sigma(I)$], w$R2$ = 0.1234 (all data), GOF = 1.064. For [**3**]$(PF_6)_2$•MeCN•Et_2O: $C_{41}H_{62}F_{12}N_7O_4P_3Pt_2RhS_2$, M_r = 1595.09, monoclinic, *C2/c*, a = 44.676(9), b = 10.133(2), c = 24.239(5) Å, β = 94.478(4)°, V = 10939(4) Å^3, Z = 8, D_{calcd} = 1.937 g cm^{-3}, 43729 total reflections, 12481 unique (R_{int} = 0.0542), $R1$ = 0.0315 [$I > 2\sigma(I)$], w$R2$ = 0.0653 (all data), GOF = 1.001.

23 Crystallographic data reported in this manuscript have been deposited with Cambridge Crystallographic Data Centre as supplementary publication nos. CCDC-1936301 and -1936302. Copies of the data can be obtained free of charge via CCDC Website.

24 A. Darchen, C. Mahé, H. Patin, *J. Chem. Soc., Chem. Commun.* **1982**, 243-245.